Preprints of the 19th World Congress
The International Federation of Automatic Control
Cape Town, South Africa. August 24-29, 2014

A New Approach of Dynamic Friction Modelling for Simulation and Observation

T. Specker * **M. Buchholz** * **K. Dietmayer** *

* *Institute of Measurement, Control and Microtechnology, University of Ulm, D-89081 Ulm, Germany (e-mail: thomas.specker@uni-ulm.de, michael.buchholz@uni-ulm.de, klaus.dietmayer@uni-ulm.de)*

Abstract: This paper presents a new dynamic friction model based on a static friction model and a linear parameter-varying first-order lowpass filter. The static model considers viscous, Coulomb, and Stribeck friction and is defined by continuous functions, yielding a smooth force transition at standstill. The adaptive filter changes its time constant dependent on the actual velocity and supplements the static model with hysteresis and memory effect. The combination of both parts offers a high accuracy in simulations using high sample rates and shows a numerically robust behaviour and a good qualitative representation of the friction for small sample rates, making it applicable for practical control tasks using an observer-based approach.

Keywords: Friction; Dry friction; Hysteresis; Dynamic modelling; Sliding surfaces.

1. INTRODUCTION

Friction is one of the most common problems in modelling and control theory. In general, it can be found in almost any mechanical system, as e. g. in bearings, linear slides, and gear boxes. Its influence on the overall system varies with the ratio between dissipative and non-dissipative forces. If the friction forces are high, they can dominate the behaviour of a system, but even if they are much smaller, they still have an undesired influence, which makes it difficult to control a system in an accurate manner.

To solve or at least minimise this problem, a lot of different approaches in friction modelling have been developed in the last 200 years, beginning with the early work of Coulomb (1821) on the effect of dry friction. Later, the work of Coulomb was refined by Stribeck (1903), adding static friction and describing the velocity dependant transition between both effects. These fundamental works were followed by many others, but even up to today, where the qualitative mechanisms are well understood, friction is still one of the most difficult and unpredictable influences in cybernetics. The combination of highly non-linear stepping behaviour with hysteresis and memory effect makes friction a variable that is hardly determinable, yet not considered the stochastic interactions as mentioned in Andersson et al. (2007).

This being the case, friction modelling is still an ongoing process, distinguished between static and dynamic modelling approaches. Static models only describe the direct link between friction and actual velocity. They neglect the hysteresis and the memory effect of friction and, therefore, are not accurate at velocity's zero crossing. A review of static model approaches based on the Coulomb and Stribeck effect is given in Wojewoda et al. (2008). Dynamic models also include the hysteresis and the memory effect of friction and, therefore, require an extension of states of the overall system model. The additional state makes the model more complex, but offers a higher model precision at velocity's zero crossing. A first dynamic model approach was presented by Dahl (1968) and refined in following publications, e.g.Canudas de Wit et al. (1995), Dankowicz (1999), and Swevers et al. (2000). As mentioned in Wojewoda et al. (2008), both static and dynamic models have their disadvantages. The simplifications make the static models not precise enough, whereas the dynamic models are often too complicated for practical engineering tasks. One disadvantage they share is the usage of stepping functions at velocity's zero crossing, which causes an unstable numerical behaviour for lower sample frequencies and applications with non-linear state observers. But especially the combination with a state observer is required to make the friction model applicable for practical control tasks.

Thus, a new dynamic friction model is derived in this contribution. Its static part describes viscous, Coulomb, and Stribeck friction and is defined by continuous functions only, making the model more robust and applicable with common observer approaches, comparable to the approach of Makkar et al. (2005). Furthermore, the proposed model also considers hysteresis and memory effect by its dynamic part. In Section 2, the model structure is explained in detail and the single features are worked out, followed by an evaluation based on a simulation of a classical stick-slip experiment in Section 3. In the stick-slip simulation, it can be shown that the model has a high precision for lower sample times, which deteriorates for higher sample times while keeping numerical stability and qualitative behaviour.

2. A NEW FRICTION MODEL

The proposed friction model is divided into two stages. Stage one is a static friction model including the viscous, Coulomb, and Stribeck effect with a smooth force transi-

tion between positive and negative velocity. The smooth transition is modelled with hyperbolic sigmoid functions in the case of dry friction and with a differentiated Gaussian function describing the Stribeck effect. All parts are modelled independently, and neglecting one of them has no influence on the behaviour of the others. The second stage adds hysteresis and memory effect using a linear parameter-varying (LPV) system in form of a first-order lowpass filter with tunable time constant and holding behaviour at standstill. A detailed description of both model stages is given in the following.

2.1 Static friction model

The basis for the new dynamic friction model is defined as a common static friction model, including viscous, Coulomb, and Stribeck friction with smoothed transitions. The different characteristics of the velocity dependent force trajectories are defined as follows.

Viscous friction, or linear damping, is rather easy to handle in modelling. The damping term

$$\tilde{F}_\mathrm{v}(v) = F_\mathrm{v}(v) = dv \tag{1}$$

with linear damping factor d describes the proportional relation between viscous friction $\tilde{F}_\mathrm{v}$ and velocity v. Since the force transition at zero velocity is smooth by nature, there is no need to customize it.

In primitive linear control applications, the overall friction is often simplified to viscous behaviour only, which offers the possibility to keep at linear control and observer approaches. But for more complex or even non-linear systems with high friction, it is not possible to achieve a satisfying control accuracy without extending the friction model with further dissipative effects, e.g. dry friction.

Coulomb friction, or dry friction, was one of the first observed friction effects, already mentioned in the work of Coulomb (1821). The value of the dry friction force is not dependent on the absolute value of velocity, but changes its sign with it. It is commonly described by

$$F_\mathrm{c}(v) = \mu F_\mathrm{n} \operatorname{sign}(v) = \hat{F}_\mathrm{c} \operatorname{sign}(v) \tag{2}$$

and depends on the normal force F_n and the coefficient of friction μ. Both together can be summarized in the peak force

$$\hat{F}_\mathrm{c} = \mu F_\mathrm{n}. \tag{3}$$

Since a switching function character given through the sign of the velocity is not desired in the proposed model approach, the sign function is approximated by a hyperbolic tangent with the transition velocity v_t, which defines the force slope at standstill. Thereby, the term for the Coulomb friction changes to

$$\tilde{F}_\mathrm{c}(v) = \hat{F}_\mathrm{c} \tanh\left(\frac{v}{v_\mathrm{t}}\right). \tag{4}$$

The difference between the original and the modified dry friction effect is shown in Fig. 1. A steeper force transition leads to a better match between approximated and original function and, therefore, to a more realistic behaviour, whereas a flatter slope guarantees a more robust numeric behaviour in simulation. A rule of thumb for choosing an appropriate value v_t is not available, since it is not only dependent on the used combination of sample time and solver, but also on the kind of state observer it is combined with later on in practical applications of the model. In general, the transition velocity has to be adapted to the given system conditions.

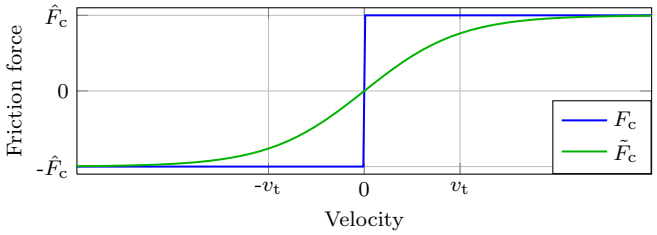

Fig. 1. Approximated Coulomb friction $\tilde{F}_\mathrm{c}$ and real Coulomb friction F_c dependant on the peak friction $\hat{F}_\mathrm{c}$ and the transition velocity v_t.

Since the dry friction model cannot explain the adhesive forces at standstill, it is supplemented by a non-linear friction force characteristic mentioned by Stribeck (1903).

Stribeck friction describes the stiction between two surfaces caused by adhesive forces and depends on various factors, such as material, geometry, and temperature. The friction force can be defined as an additional part to dry friction in the general form of

$$F_\Delta(v) = \left(\hat{F}_\mathrm{s} - \hat{F}_\mathrm{c}\right) g(v) \operatorname{sign}(v) = \hat{F}_\Delta g(v) \operatorname{sign}(v) \tag{5}$$

with the non-linear function $g(v)$, describing the decay characteristics of the Stribeck curve, and the additional force amplitude

$$\hat{F}_\Delta = \hat{F}_\mathrm{s} - \hat{F}_\mathrm{c}, \tag{6}$$

consisting of the Stribeck peak force $\hat{F}_\mathrm{s}$ and the peak force of Coulomb friction. There are many possible definitions of $g(v)$, a review of the most common approaches is given in Wojewoda et al. (2008), comprising exponential, generalized exponential, Gaussian, Laurentzian, and Popp-Stelter function behaviour. There are no suitable models to calculate the dominating parameters which characterizes the stiction behaviour, e.g. the Stribeck velocity v_s for Gaussian approaches. Therefore, the parameter values have to be identified in experimental setups.

In the proposed model, an adapted version of the Gaussian bell approach

$$g(v) = \mathrm{e}^{-\left(\frac{v}{v_\mathrm{s}}\right)^2} \tag{7}$$

is used and modified to

$$\tilde{g}(v) = \frac{v}{v_\mathrm{sp}} \mathrm{e}^{-\left(\frac{v}{\sqrt{2}v_\mathrm{sp}}\right)^2 + \frac{1}{2}}, \tag{8}$$

where the Stribeck peak velocity v_sp defines the friction decay, but is not equal to the Stribeck velocity v_s. In contrast to $g(v)$, the adapted function $\tilde{g}(v)$ already includes the sign function. The difference between both functions is shown in Fig. 2 for a peak velocity v_sp half the size of the Stribeck velocity v_s. The flatter the slope at zero crossing is chosen, the more the peak of the approximated friction moves away from its usually position at zero velocity. If a very flat slope is required, it might be better to neglect the Stribeck effect, otherwise there is not only a wrong model behaviour at standstill, but also a peak of friction at higher velocities which falsifies the model.

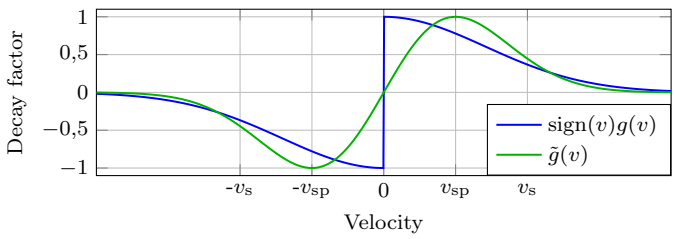

Fig. 2. Behaviour of Stribeck friction for a Gaussian bell function $g(v)$ with sign step and decay factor v_s and for an adapted Gaussian function $\tilde{g}(v)$ with smooth transition dependent on the peak velocity v_{sp}.

If the Stribeck effect is not omitted, the additional force amplitude $\hat{F}_\Delta$ has to be adapted as well. Because the Coulomb force $\tilde{F}_c$ is not constant any more, the gap between the Stribeck peak and the dry friction force widens at the velocity v_{sp} and, therefore, has to be considered by

$$\hat{\tilde{F}}_\Delta = \hat{F}_s - \hat{F}_c \tanh\left(\frac{v_{sp}}{v_t}\right) - d v_{sp}. \tag{9}$$

For the sake of completeness, the viscous friction at v_{sp} is subtracted as well, even if its value is not significant for small velocities, where the force peak is suspected.

In total, the combination of the adapted Gaussian bell (8) and the additional peak force (9) yields the modified Stribeck force

$$\tilde{F}_\Delta(v) = \hat{\tilde{F}}_\Delta \tilde{g}(v). \tag{10}$$

By adding up all three described friction effects, the dissipative overall force of the smoothed static friction model is

$$\tilde{F}_\Sigma(v) = \tilde{F}_v(v) + \tilde{F}_c(v) + \tilde{F}_\Delta(v), \tag{11}$$

which is depicted in Fig. 3 together with each single characteristics and a comparison with the common friction force

$$F_\Sigma(v) = F_v(v) + F_c(v) + F_\Delta(v). \tag{12}$$

A good function approximation for small sample times can be achieved by using the ratio

$$v_s \approx 2 v_{sp} \approx 4 v_t, \tag{13}$$

where, beginning at a velocity of $v \approx v_{sp}$, the trajectories $F_\Sigma(v)$ and $\tilde{F}_\Sigma(v)$ are almost equal. For practical applications with higher sample times, v_t and v_{sp} might be chosen greater than v_s to maintain numerical stability.

The resulting loss of accuracy can be compensated by an observer.

2.2 Hysteresis and memory effect

The static friction model described in the previous paragraph is not able to reproduce the dynamic friction behaviour. There is not only a loss of precision by making the model continuously differentiable, it also yields zero force at standstill because of the lack of hysteresis and memory effect.

For dynamic systems, it is rather easy to achieve hysteresis by using a linear lowpass filter that delays the force to the velocity. Following other dynamic friction model approaches, e.g. Canudas de Wit et al. (1995) and Dankowicz (1999), the used filter should not contain more than one state to keep the model simple. Therefore, a linear first-order lag element with the transfer function

$$G(s) = \frac{1}{T_1 s + 1}, \tag{14}$$

the time constant T_1, and a gain of one is used. If the lag element is connected in series after the static friction model, the overall behaviour changes as shown in Fig. 4. Based on the increasing damping behaviour for higher frequencies, the lag element widens the hysteresis and the force at standstill changes to a value almost as high as the Coulomb force. Furthermore, the friction's peak force decreases, which is another characteristic of the Stribeck effect that was reported in the works of Canudas de Wit et al. (1995), Swevers et al. (2000), and Wojewoda et al. (2008).

Compared to the positive effects of lowpass filtering for higher velocity rates, there is only a poor improvement for low or zero dynamics. The only way to enhance the model for small accelerations is increasing the time constant, changing it even up to infinity for static cases. But in turn, this leads to an undesired strong damping behaviour at higher dynamics. To solve this conflict, a non-linear filter is used that combines the different tasks by varying the time constant dependent on the actual velocity.

The approach applied here is based on a linear parameter-varying filter. The filter parameters have to be changed in such a way that the time constant is small at high velocities, growing at low velocities, and infinity at standstill. Apart from this, the gain value shall remain constant at

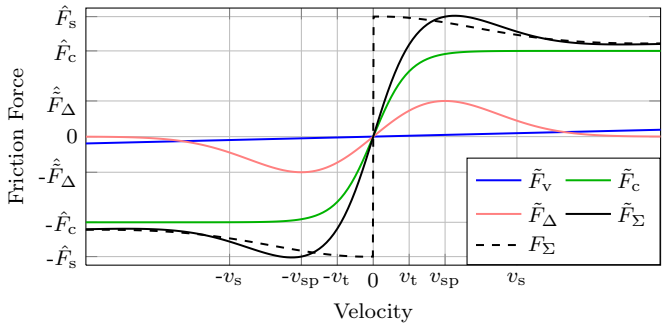

Fig. 3. Viscous force $\tilde{F}_v$, Coulomb force $\tilde{F}_c$, additional Stribeck force $\tilde{F}_\Delta$, and overall force $\tilde{F}_\Sigma$, in contrast to the common friction force F_Σ.

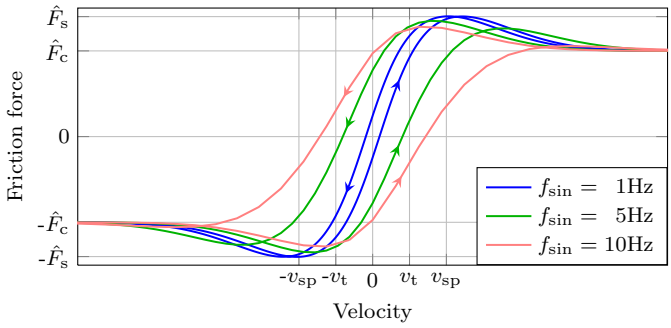

Fig. 4. Friction forces for sine-shaped velocities with amplitude $0.1\frac{\text{m}}{\text{s}}$ and a linear filter with time constant $T_1 = 3\text{ms}$.

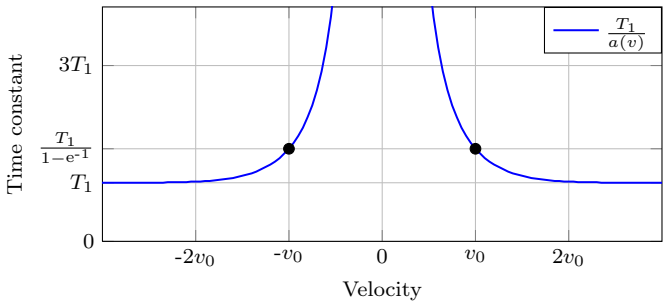

Fig. 5. Varying lowpass time constant as a function of the sliding speed with minimal time constant T_1 and edge velocity v_0.

one. Therefore, the linear first-order lag element is supplemented by a velocity dependent parameter $a(v)$, yielding the linear parameter-varying transfer function

$$\tilde{G}(s) = \frac{1}{\frac{T_1}{a(v)}s + 1} = \frac{a(v)}{T_1 s + a(v)}. \tag{15}$$

The adaption factor $a(v)$ is defined by another Gaussian bell

$$a(v) = 1 - \mathrm{e}^{-\left(\frac{v}{v_0}\right)^2} \tag{16}$$

with the edge velocity v_0 effecting the overall time constant as shown in Fig. 5. Beginning at $v = v_0$, the time constant grows rapidly and even reaches infinity for $v = 0$.

2.3 Overall Friction Model

Summarizing the static friction and the parameter-varying filter, the complete dynamic friction model results in the differential equation

$$\dot{F}_{\mathrm{fr}}(v) = \frac{1 - \mathrm{e}^{-\left(\frac{v}{v_0}\right)^2}}{T_1} \left(\tilde{F}_{\Sigma}(v) - F_{\mathrm{fr}}(v) \right), \tag{17}$$

which is depicted in Fig. 6 as a block diagram. In case of $v \gg v_0$, the equation changes to

$$\dot{F}_{\mathrm{fr}}(v) = \frac{1}{T_1} \left(\tilde{F}_{\Sigma}(v) - F_{\mathrm{fr}}(v) \right), \tag{18}$$

whereas at standstill, it simplifies to

$$\dot{F}_{\mathrm{fr}}(v) = 0. \tag{19}$$

Being the force derivative equal to zero, the filter behaves as a hold element, i.e. the overall model includes the desired memory effect by holding the force value that occurs at the last moment of motion. An example of the memory effect is shown in Fig. 7. Between 0.8 s and 1 s, both velocity trajectories show standstill, but the related friction force is held at different values dependent on

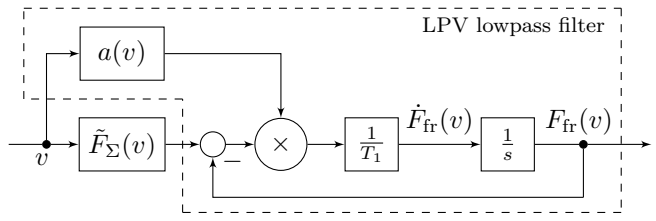

Fig. 6. Block diagram of the dynamic friction model with a serial connection of the static friction model $\tilde{F}_{\Sigma}$ and the adaptive first order lowpass filter.

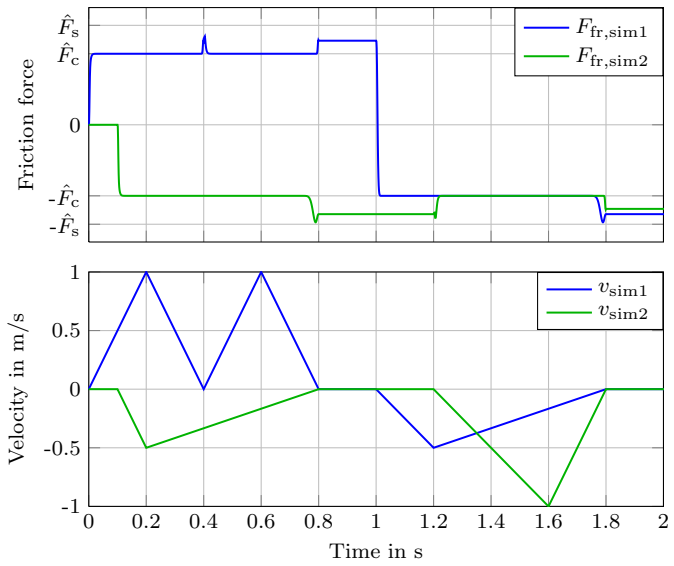

Fig. 7. Friction forces $F_{\mathrm{fr,sim}}$ with hysteresis and memory effect dependent on the velocity trajectories v_{sim}.

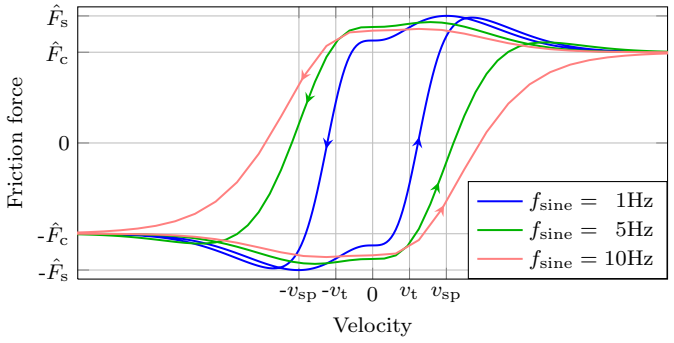

Fig. 8. Friction forces for sine-shaped velocities with amplitude $0.1\frac{\mathrm{m}}{\mathrm{s}}$ and parameter-varying filter with time constant $T_1 = 3\mathrm{ms}$ and edge velocity $v_0 = v_{\mathrm{sp}}$.

the former sign of velocity. In addition, there are other occurring friction characteristics that can be seen, e.g. the transition between dry friction and adhesion in $F_{\mathrm{fr,sim1}}$ at 0.4 s and the initialisation of $F_{\mathrm{fr,sim2}}$ at 0.1 s. Up to this point, the memory of the linear parameter-varying filter has no former information and remains at its initial value zero.

If the hysteresis caused by linear filtering, as shown in Fig. 4, is compared to the hysteresis modeled with the linear parameter-varying filter, which is shown in Fig. 8, there are remarkable differences. The hysteresis gap of the non-linear approach is much broader, while the slope of the transition remains unchanged. In other words, the delay has only to be chosen large enough to maintain numerical stability, and the friction behaviour for low dynamics still can be reproduced.

3. SIMULATION EXAMPLE

As a first evaluation approach for the new friction model, a classical stip-slick experiment is chosen as depicted in Fig. 9. It is made up of a mass m, pulled by a spring with spring constant k that is moving with a constant velocity v_{spr}. At the beginning, the adhesion keeps the mass at

standstill and the distance between the mass position s_m and the spring position s_spr increases. This leads to a growing tension of the spring and thus to a higher force

$$F_\mathrm{spr} = k\,(s_\mathrm{spr} - s_\mathrm{m}) \tag{20}$$

that is proportional to the spring constant and effecting the mass directly. If the spring force has increased to the level of the adhesive force, the mass breaks free and starts to slide. This causes an abrupt decrease of the friction force to the value of dry friction and therefore to an additional acceleration. At the point where the mass moves faster than the spring, the spring tension weakens. If it subsides to a level lower than Coulomb force, the mass decelerates and returns to standstill, otherwise the mass follows the spring position with equal velocity and constant position delay.

The mathematical model of the stick-slip experiment consists of two coupled differential equations, one already shown in (17), describing the dynamic behaviour of the friction force, and

$$m\ddot{s}_\mathrm{m} = k\,(s_\mathrm{spr} - s_\mathrm{m}) - F_\mathrm{fr}(\dot{s}_\mathrm{m}), \tag{21}$$

characterizing the dynamics of the mass movement, with the spring position s_spr as model input and the mass position s_m as output.

The results presented here are simulated with Simulink® using a fourth order Runge-Kutta method with fixed sample time for solving the differential equations. The simulation is done for two different sample times to show the mentioned advantages of the friction model.

As an example for the precision that can be reached, the sample time is chosen to $T_\mathrm{s} = 0.1\,\mathrm{ms}$. Due to the fact that such a small sample time cannot be provided in most practical control tasks, another simulation is presented, which is executed with a sample time of $T_\mathrm{s} = 10\,\mathrm{ms}$. If the model shows a robust and qualitative correct behaviour for the second case, it should be possible to apply the model in practice as well.

The simulation parameters are distinguished between constants and variables and are listed in Table 1 and Table 2. While mass, spring constant, and the peak forces remain unchanged, the friction properties of the new model have to be adapted to the used sample times. Since one sample frequency is a hundred times faster than the other one, the time constant T_1 and the characteristic velocities v_sp, v_t, and v_0 are also varying with the same ratio.

In the regarded sequence, the spring position moves with constant velocity $v_\mathrm{spr} = 0.1\,\frac{\mathrm{m}}{\mathrm{s}}$ for five seconds and then stops abruptly. The simulation results for the occurring forces are depicted in Fig. 10, and the mass dynamics, described by position and velocity are shown in Fig. 11.

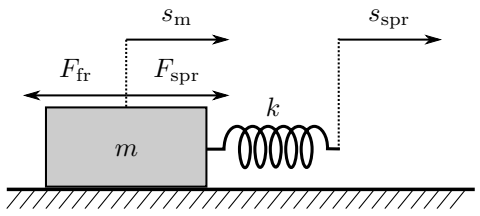

Fig. 9. Benchmark model for stick-slip experiments, pulling a mass by a spring with constant velocity v_spr.

Table 1. Constant simulation parameters

m in kg	k in $\frac{\mathrm{N}}{\mathrm{m}}$	$\hat{F}_\mathrm{s}$ in N	$\hat{F}_\mathrm{c}$ in N	d in $\frac{\mathrm{Ns}}{\mathrm{m}}$
0.1	10	1.4	1	0.1

Table 2. Varying simulation parameters

T_s in ms	v_t in $\frac{\mathrm{m}}{\mathrm{s}}$	v_sp in $\frac{\mathrm{m}}{\mathrm{s}}$	v_0 in $\frac{\mathrm{m}}{\mathrm{s}}$	T_1 in s
0.1	0.00005	0.0001	0.0001	0.0003
10	0.05	0.01	0.01	0.03

The qualitative behaviour of both simulations is similar, but they show a distinct difference with regard to quantity.

The simulation with $T_\mathrm{s} = 0.1$ ms shows a realistic slip-stick behaviour. In cases of expected standstill, there is no remarkably drift in the position trajectory. The same effect can be seen in the velocity curve as well. In the force trajectory, all characteristic parts of friction appear, the increasing force at standstill, the transition between Stribeck and dry friction, and the viscous friction in cases of motion. Furthermore, the overall force shows a constant value beginning at five seconds, enforced by the holding character of the parameter-varying filter.

The presented results are similar to those of the LuGre model described in Canudas de Wit et al. (1995). The LuGre model, based on the works of Canudas de Wit et al. (1993), Canudas de Wit et al. (1995), and Olsson (1996), is one of the most established friction models. Therefore, it can be concluded that the new model has a high precision for high sample frequencies.

Regarding the simulation results for $T_\mathrm{s} = 10\,\mathrm{ms}$, a slightly lower accuracy of the model is recognisable. At times where the mass should remain in its position, a slow motion has to be noticed. The drift of mass, observable from position and velocity in Fig. 11, is caused by the flatter slope of the underlying static friction model as well as the slower

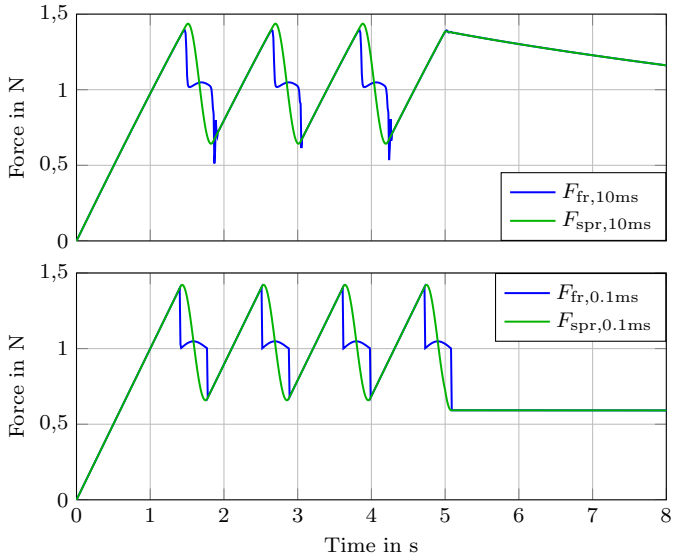

Fig. 10. Friction forces F_fr and spring forces F_spr for stick-slip simulation using different sample times.

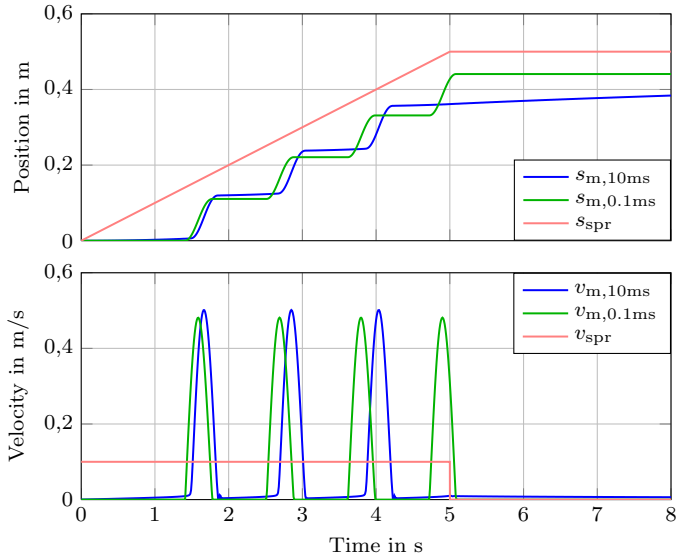

Fig. 11. Mass position s_m and spring position s_{spr} (upper figure) and related velocities v_m and v_{spr} (lower figure) for stick-slip simulation using different sample times.

dynamics of the following filter. Thus, the friction force is delayed in comparison to the spring force and an exact compensation is not possible any more.

Caused by the drift of position, the tension of the spring increases more slowly, leading to a delay of the breaking point of adhesion and resulting in a lower frequency of the stick-slip effect, as can be seen in Fig. 10. Furthermore, the mentioned delay also effects a slow drift of s_m towards s_{spr} at the end of the simulation. This implies that the filter adaption is not able to move the time constant to infinity and reaching the desired holding behaviour of the memory effect. However, the quantitative behaviour of the model is still reasonable and good enough to be used in an observer, which would compensate some of the differences, and the simulation is numerically stable, which is a significant advantage over other model approaches.

4. CONCLUSION

In this contribution, a new approach for a dynamic friction model has been presented. In contrast to other friction models, e.g. the LuGre model, it is defined by continuous functions only. This offers a better numeric stability, but also leads to an approximation error in the underlying static friction model, which consists of the viscous, Coulomb, and Stribeck effect.

To improve the model accuracy and adding features like hysteresis and memory effect, a linear parameter-varying first-order lag element is connected in series, behaving as a lowpass filter with varying time constant. This makes it possible to delay the friction force towards the velocity, achieving hysteresis as well as acting as a hold element in cases of standstill. By applying the adaptive filter on the static friction model, it is even possible to compensate for the negative effects caused by smoothing the transition at zero velocity.

The new model has been evaluated by simulation with a classical stick-slip experiment. For high sample frequencies, the new model shows a high precision which is comparable to reputable models while remaining numerically stable for lower frequencies. To keep stability, a slight impairment in accuracy has to be accepted, but the qualitative characteristics are still good.

Since the model combines the features of being defined by continuous functions and maintaining stability for small sample rates, it is possible to apply it in practical applications. This has to be tested in combination with nonlinear state observers and different controller approaches. Particularly interesting is the usage of the new model for friction compensation, where both, a high dynamic behaviour and an accurate estimation are necessary.

ACKNOWLEDGEMENTS

The authors thank the German Federal Ministry of Economics and Technology for supporting this work through the Central Innovation Program SME within the project KF2648502NT1.

REFERENCES

Andersson, S., Söderberg, A., and Björklund, S. (2007). Friction models for sliding dry, boundary and mixed lubricated contacts. *Tribology International*, 40, 580–587.

Canudas de Wit, C., Olsson, H., Åström, K., and Lischinsky, P. (1993). Dynamic friction models and control design. In *Proceedings of the 1993 American Control Conference, San Francisco, California.*

Canudas de Wit, C., Olsson, H., Åström, K., and Lischinsky, P. (1995). A new model for control of systems with friction. *IEEE Transactions on Automatic Control*, 40, 419–425.

Coulomb, C. (1821). *Théorie des machines simple (Nouv. éd.)*. Bachelier.

Dahl, P. (1968). A solid friction model. Technical Report TOR-0158(3107-18), The Aerospace Corporation, El Segundo, CA.

Dankowicz, H. (1999). On the modeling of dynamic friction phenomena. *Z. Angew. Math. Mech.*, 79, 399–409.

Makkar, C., Dixon, W., Sawyer, W., and Hu, G. (2005). A new continuously differentiable friction model for control systems design. In *Proceedings of the 2005 IEEE/ASME International Conference on Advanced Intelligent Mechatronics, Monterey, California.*

Olsson, H. (1996). *Control Systems with Friction.* Ph.D. thesis, Department of Automatic Control, Lund Institute of Technology, Lund, Sweden.

Stribeck, R. (1903). *Wesentliche Eigenschaften der Gleit- und Rollenlager.* Springer.

Swevers, J., Al-Bender, F., Ganseman, C., and Prajogo, T. (2000). An integrated friction model structure with improved presliding behaviour for accurate friction compensation. *IEEE Transactions on Automatic Control*, 45, 675–686.

Wojewoda, J., Stefanski, A., Wiercigroch, M., and Kapitaniak, T. (2008). Hysteretic effects of dry friction: modelling and experimental studies. *Phil. Trans. R. Soc. A*, 366, 747–765.